

Timeliness in NextG Spectrum Sharing under Jamming Attacks with Deep Learning

Maice Costa and Yalin E. Sagduyu
Nexcepta, Gaithersburg, MD, USA
{mcosta, ysagduyu}@nexcepta.com

Abstract—We consider the communication of time-sensitive information in NextG spectrum sharing where a deep learning-based classifier is used to identify transmission attempts. While the transmitter seeks for opportunities to use the spectrum without causing interference to an incumbent user, an adversary uses another deep learning classifier to detect and jam the signals, subject to an average power budget. We consider timeliness objectives of NextG communications and study the Age of Information (AoI) under different scenarios of spectrum sharing and jamming, analyzing the effect of transmit control, transmit probability, and channel utilization subject to wireless channel and jamming effects. The resulting signal-to-noise-plus-interference (SINR) determines the success of spectrum sharing, but also affects the accuracy of the adversary’s detection, making it more likely for the jammer to successfully identify and jam the communication. Our results illustrate the benefits of spectrum sharing for anti-jamming by exemplifying how a limited-power adversary is motivated to decrease its jamming power as the channel occupancy rises in NextG spectrum sharing with timeliness objectives.

I. INTRODUCTION

The increasing demand for spectrum resources has led to a critical need for innovative strategies to address the challenges posed by spectrum scarcity [1]–[3]. As traditional frequency bands become congested and the spectrum becomes a valuable and limited commodity, it has been imperative to explore novel approaches to optimize spectrum utilization. One promising avenue is spectrum sharing, where multiple transmitters co-exist within the same frequency band, aiming to enhance overall spectral efficiency. To that end, an emerging example is spectrum sharing in the 3.5GHz Citizens Broadband Radio Service (CBRS) band, where the spectrum band needs to be shared with the radar that serves as the incumbent user.

The urgency of addressing spectrum scarcity is further underscored by the growing importance of timely communication in various applications, ranging from mission-critical first responder and disaster recovery operations to emerging technologies like the Augmented Reality (AR), Virtual Reality (VR), Extended Reality (XR), Vehicle-to-Everything (V2X), Internet of Things (IoT), and smart cities. Information freshness in timely communications is essential in NextG applications where real-time data dissemination is of paramount importance [4]. For example, V2X communication, essential for the advancement of smart transportation systems, requires timely exchange of information between vehicles and infrastructure to enhance road safety and traffic efficiency. Similarly, the diverse ecosystem of IoT applications, spanning

from smart cities to industrial automation, relies on timely data updates to make informed decisions and take timely actions. Age of Information (AoI) denoting the time elapsed since the generation of the last received update provides the mathematical framework to assess the timeliness in information transfer [5]. A lower AoI indicates that the delivered data is not only current but also aligns seamlessly with the real-time requirements of the emerging NextG applications. This alignment, in turn, amplifies the efficiency and responsiveness of real-time experiences, optimizing decision-making processes and enabling prompt actuation based on the most recent data.

The pursuit of timeliness in NextG communication is not without its challenges. Given the open and shared nature of wireless communications, NextG is susceptible to new threats and exploits [6]. The use of adversarial machine techniques to prevent eavesdroppers from detecting ongoing transmissions has been discussed in [7]–[9]. The outcomes of eavesdropping can be used consequently for jamming the ongoing transmissions. To support time-sensitive applications, timely communications has been considered under the objectives of covertness [10]–[13] and anti-jamming [14]–[16].

This paper studies the intricate interplay between spectrum sharing, timeliness of communications, and the vulnerability to eavesdropping and jamming attacks. Our results aim to unravel the dynamics of this complex environment, where the classification performance of the deep learning-based system influences the selection of jamming power by the adversary. Recognizing the constraints of an adversary with limited resources, we investigate the average AoI as a key metric to quantify the impact of our proposed approach. Importantly, we demonstrate the advantages of spectrum sharing, showcasing how an adversary with a restricted power budget is incentivized to reduce its jamming power as the channel occupancy increases. The main contributions of this paper include:

- The analytical characterization of AoI in the proposed scenario with spectrum sharing in the presence of an adversary, considering the detection errors that may occur in spectrum sensing and eavesdropping.
- A discussion about the use of deep-learning based classifiers both by the transmitter and by the adversary to guide the decisions to transmit according to the goals of each party. We include the effects of the wireless channel, as well as design parameters as the packet size. We show that smaller packet sizes decrease detection accuracy, and may result in smaller average AoI in a

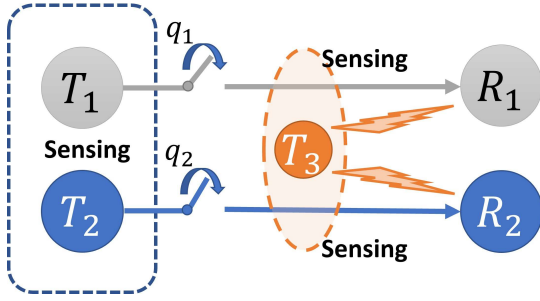


Fig. 1. Network system model.

scenario with scarce spectrum resources and the presence of an adversary.

- A thorough investigation of the effects of channel occupancy on the selected jamming power and resulting average AoI. We show the adjustment of jamming power according to spectrum utilization, and highlight the reduction of the AoI when more spectrum resources are available or less jamming power is used to cause interference.

The remainder of the paper is organized as follows. Sec. II describes the system model. Sec. III evaluates the performance in terms of average AoI and jamming power in spectrum sharing. Sec. IV concludes the paper.

II. SYSTEM MODEL

A. Communication Model

We consider a communication network setting with two transmitter-receiver pairs sharing the spectrum resources. We denote with T_1 and T_2 the transmitter nodes, and assume that T_1 (incumbent or primary user) has absolute priority to use the spectrum, while T_2 (secondary user) should listen to the channel and transmit only if T_1 is silent. Receiver nodes are denoted with R_1 and R_2 for incumbent and secondary users, respectively. Communication is assumed to take place in a hostile environment where an active adversary (T_3) can potentially eavesdrop and jam the signal of both transmitters. The network model is illustrated in 1.

We assume that at each time slot, T_1 will occupy the spectrum with probability q_1 independent of other time slots. The secondary user T_2 will use a deep learning classifier to decide about the presence of the incumbent at each time slot. This detection task is subject to Type 1 (false positive) and Type 2 (false negative) errors. Missdetection probability is denoted with p_m and false alarm probability is denoted with p_f . At a given time slot, we denote with q the probability that the secondary has packets to transmit, but it will act on its intention only if the channel is believed to be available. We denote with q_2 the probability of a transmission from T_2 , where

$$q_2 = [(1 - q_1)(1 - p_f) + q_1 p_m]q. \quad (1)$$

The eavesdropper T_3 also uses a deep learning classifier to decide about channel occupancy. We assume that it will emit

an interfering signal if and only if it detects that the channel is occupied (by either transmitter). The set of active nodes impacts the classification accuracy, and we denote the errors with p_m^i and p_f^i when the transmitter T_i is active, and with p_m^{12} and p_f^{12} when both the transmitters are active. We assume that the secondary transmitter is capable of making a decision before the eavesdropper, so T_2 only considers the activity of T_1 when deciding to transmit, while T_3 considers the activity of both T_1 and T_2 . It is reasonable to expect that $p_m^{12} \leq p_m^i$ and $p_f^{12} \leq p_f^i$, for $i \in \{1, 2\}$, as the SNR increases when combining the transmit powers of both T_1 and T_2 .

Transmit powers are denoted with P_i , $i \in \{1, 2, 3\}$. We assume that transmissions take place using fixed and independent resource blocks with binary phase shift keying (BPSK) modulation and transmissions are subject to Rayleigh fading plus Gaussian noise of average power σ^2 . We assume that channels between two nodes are independent. The corresponding received power at another node k is $R(i, k) = P_i g(i, k) h(i, k)$, where $g(i, k)$ represents a path gain that may include shadowing and attenuation as a function of distance between nodes, or antenna gain. For the purposes of this work, we assume $g(i, k)$ to remain constant. $h(i, k)$ represents the small scale fading. In the case of Rayleigh fading, the signal envelope follows a Rayleigh distribution, while the received power follows an exponential distribution of parameter $h(i, k)$.

We assume that a transmission is successful if the signal-to-noise-plus-interference (SINR) is above a given threshold γ_{min} . Let \mathcal{A} denote the powerset of $\{1, 2, 3\}$. For a given set $A \in \mathcal{A}$ of active nodes transmitting simultaneously in the same channel (and causing interference to each other), the probability that the intended receiver can successfully decode the signal is given by

$$S_i(A) = \exp - \frac{\gamma_{min} \sigma^2}{P_i g(i, i) h(i, i)} \times \prod_{j \in A \setminus \{i\}} \left[1 + \gamma_{min} \frac{P_j g(j, i) h(j, i)}{P_i g(i, i) h(i, i)} \right]. \quad (2)$$

The probability of a successful transmission for the pair of T_i and R_i , $i \in \{1, 2\}$, is calculated averaging over all possible sets of active nodes,

$$S_i = \sum_{A \in \mathcal{A}} S_i(A) \mathbb{P}(A), \quad (3)$$

where we assume $P_i = 0$ if T_i is not active to simplify notation and average over all sets. The term $\mathbb{P}(A)$ represents the probability of a given set of active nodes A , expressed as a function of the transmit probabilities for each type of node. For example, when the incumbent transmitter T_1 is silent, while the secondary transmitter T_2 is active and the jammer T_3 is active, $A = \{2, 3\}$. We express all the events with an active

secondary user and the respective probabilities as

$$\mathbb{P}(A = \{1, 2, 3\}) = q_1 p_m q (1 - p_m^{12}), \quad (4)$$

$$\mathbb{P}(A = \{2, 3\}) = (1 - q_1)(1 - p_f)q(1 - p_m^2), \quad (5)$$

$$\mathbb{P}(A = \{1, 2\}) = q_1 p_m q p_m^{12}, \quad (6)$$

$$\mathbb{P}(A = \{2\}) = (1 - q_1)(1 - p_f)q p_m^2. \quad (7)$$

B. Adversary Model

We assume an adversary (T_3) that listens to the communication channel and uses a deep learning classifier to decide about the presence of a signal to interfere with. When a signal is detected, T_3 actively jams the signal with the objective to increase the interference level and disrupt the communication in the channel. We assume that the adversary cannot distinguish between the incumbent or secondary transmissions, so the decision to jam is triggered by any activity in the channel. We assume that T_3 never transmits an interfering signal when it believes the channel is idle, but the output of the classifier is imperfect, with Type 1 (false positive) and Type 2 (false negative) errors. The accuracy of the classification task depends on the transmitted signal and the channel quality. We assume that transmit power and/or channel conditions may be different between nodes in the network. We denote with q_3 the probability that the jammer will be activated. We express all the events with an active jammer and the respective probabilities as

$$\mathbb{P}(A = \{1, 2, 3\}) = q_1 p_m q (1 - p_m^{12}), \quad (8)$$

$$\mathbb{P}(A = \{2, 3\}) = (1 - q_1)(1 - p_f)q(1 - p_m^2), \quad (9)$$

$$\mathbb{P}(A = \{1, 3\}) = q_1((1 - p_m) + p_m(1 - q))(1 - p_m^1), \quad (10)$$

$$\mathbb{P}(A = \{3\}) = (1 - q_1)(p_f + (1 - p_f)(1 - q))p_f^{12}. \quad (11)$$

The probability of an active jammer is given by the sum of probabilities of the four events, as

$$q_3 = \sum_{\{A \in \mathcal{A}: A \supseteq \{3\}\}} \mathbb{P}(A). \quad (12)$$

The decision to jam the detected signal is subject to an average jamming power constraint \bar{P}_{max} that represents the concern with a limited power budget. The average power \bar{P}_3 satisfies $\bar{P}_3 \leq \bar{P}_{max}$, with $\bar{P}_3 = P_3 q_3$.

C. Status Updating Model

We assume that the communication between T_i and R_i concerns time-sensitive information, so the transmitter obtains the packet immediately before transmission. At the receiver R_i , the AoI evolves as

$$\Delta_i(t+1) = \begin{cases} 1 & \text{w.p. } S_i, \\ \Delta_i(t) + 1 & \text{w.p. } 1 - S_i. \end{cases} \quad (13)$$

This process can be described as a Discrete Time Markov Chain (DTMC) [17]. At state k the chain can either transition to state $k+1$, when no packet is received, or to state 1, when a packet is received and AoI is updated. The steady state

distribution is $\pi_k^{\Delta_i} = (1 - S_i)^{k-1} S_i$, for all k . The average AoI is calculated as

$$\begin{aligned} \bar{\Delta}_i &= \sum_{k=1}^{\infty} k \pi_k^{\Delta_i} \\ &= \sum_{k=1}^{\infty} k (1 - S_i)^{k-1} S_i \\ &= \frac{S_i}{1 - S_i} \sum_{k=1}^{\infty} k (1 - S_i)^k \\ &= \frac{S_i}{1 - S_i} \frac{1 - S_i}{S_i^2}. \end{aligned} \quad (14)$$

As a result, we have $\bar{\Delta}_i = 1/S_i$.

III. PERFORMANCE ANALYSIS

A. Signal Detection

Spectrum data characteristics can be effectively captured by deep learning, providing higher accuracy in wireless signal classification compared to simpler machine learning models or other statistical methods such as energy detection [18], [19]. We assume that the secondary user uses a convolutional neural network (CNN) for spectrum sensing, while the adversary uses a feedforward neural network (FNN). We consider Glorot uniform initializer, Adam optimizer, and categorical cross entropy loss function to implement a binary classifier with labels ‘Signal’ vs. ‘No Signal’ for these deep learning models. We show the deep neural network architectures in Table I.

Fig. 2 shows the classification accuracy for CNN and FNN models with packets of 64 I/Q samples. Overall, CNN outperforms FNN in terms of classification accuracy that depends on the SNR in the channel between the transmitter and the adversary. We also note that the detection accuracy increases with the packet size as we consider packets with 16, 32, 64 and 128 I/Q samples. The increased accuracy comes at the expense of large number of parameters for the classifier. The number of parameters increases from 3,230 to 17,566 for FNN and from 37,306 to 266,682 for CNN, when we increase packet size from 16 to 128. When fixing the packet size, we adopt the value of 64 I/Q samples, with 9,374 trainable parameters for FNN and 135,610 trainable parameters for CNN.

B. Communication Timeliness

We consider $h(i, k) = 1$ and $g(i, k) = 2^{-4}$ to represent an attenuation coefficient over a distance. The SNR is assumed

TABLE I
DEEP NEURAL NETWORK ARCHITECTURES.

FNN	CNN
Dense (64, ReLU)	Conv2D ((1,3), ReLU)
Dropout (0.1)	Flatten
Dense (16, ReLU)	Dense (32, ReLU)
Dropout (0.1)	Dropout (0.1)
Dense (4, ReLU)	Dense(8, ReLU)
Dropout (0.1)	Dropout (0.1)
Dense (2, SoftMax)	Dense (2, SoftMax)

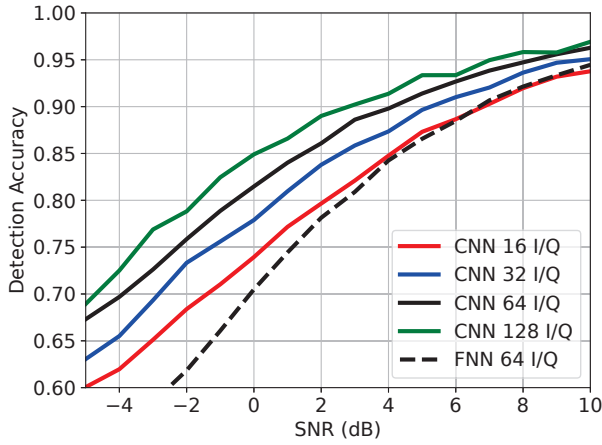


Fig. 2. Classifier accuracy versus SNR and effect of number of I/Q symbols per packet.

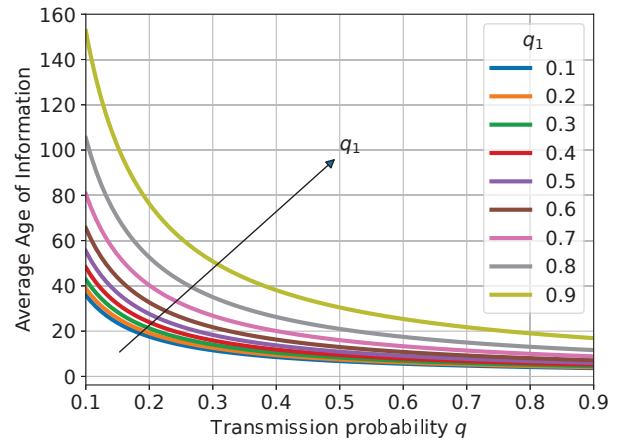


Fig. 4. Average AoI versus probability that secondary user intends to transmit (subject to spectrum sensing) varying q_1 .

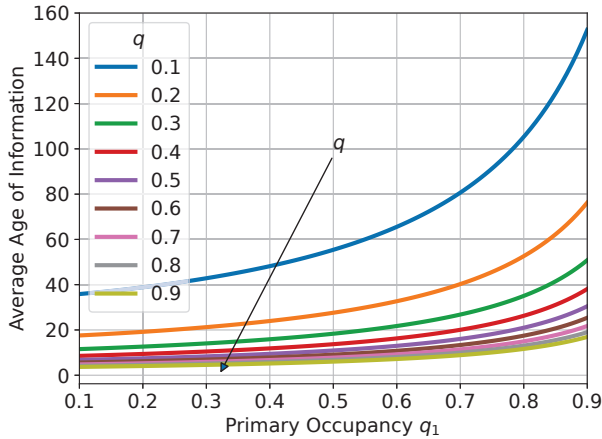


Fig. 3. Average AoI versus incumbent channel occupancy varying the probability that secondary has packets, q .

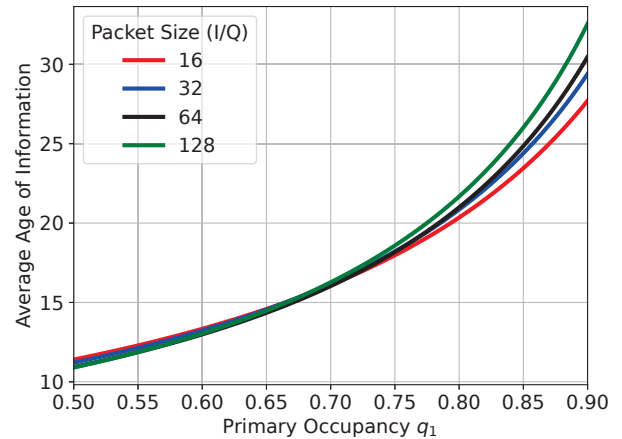


Fig. 5. Average AoI versus incumbent channel occupancy varying packet size (in I/Q samples) with $q = 0.5$.

to be $\gamma = 0$ dB for the purposes of signal detection. We assume a CNN classifier is used for spectrum sensing by the transmitter, while the adversary uses a FNN classifier. Unless otherwise stated, we use packets of 64 I/Q samples. When both the incumbent and the secondary user are transmitting, the jammer observes a 3 dB increase in SNR and the detection accuracy is increased accordingly. Fig. 3 shows the average AoI at the secondary receiver versus the probability of an incumbent transmission q_1 . The presence of the incumbent should prevent the secondary user from transmitting, except for the misdetection events. As a result, the AoI increases with q_1 . When incumbent occupancy is less than 50%, its effect on AoI is reduced. Also, the effect of a large q_1 is more prominent when the secondary transmission attempts are sparse.

Fig. 4 presents the average AoI versus the probability that the secondary node intends to transmit. Note that this is not the secondary transmit probability q_2 , which also depends on q_1 , but the independent variable q , which can be thought of as the rate that packets are generated at the transmitter. In

the unconstrained case, more attempted transmissions translate into higher success probability and hence smaller AoI. If transmissions were constrained, by a power budget for example, these results indicate that limited gain is obtained when increasing the packet generation beyond 0.4. Higher rates are particularly desirable when spectrum is scarce, meaning that the secondary user should take advantage of a transmission opportunity when one arrives.

The effect of packet size is illustrated in Fig. 5, assuming the transmitter is activated with probability $q = 0.5$, if the spectrum is classified to be available. Packet size is more relevant when spectrum resources are scarce, and the results suggest that small packets yield smaller AoI in that case, when q_1 is large. In this scenario, the small packets result in smaller detection probability by the jammer, hence reducing interference. On the other hand, when the probability of incumbent transmission is small, the behavior is reversed, and larger packet sizes result in smaller average AoI.

The effect of power control is illustrated in Fig. 6, where we

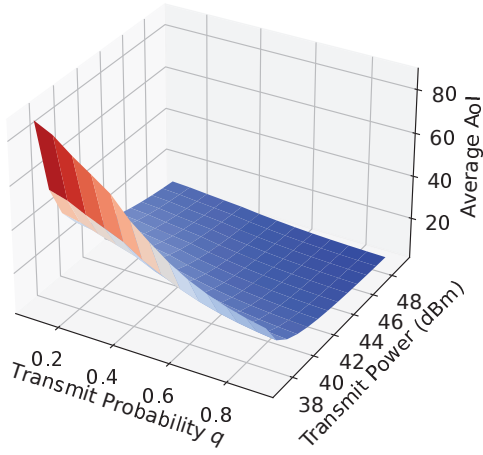


Fig. 6. Average AoI versus transmit power and transmit probability for secondary user.

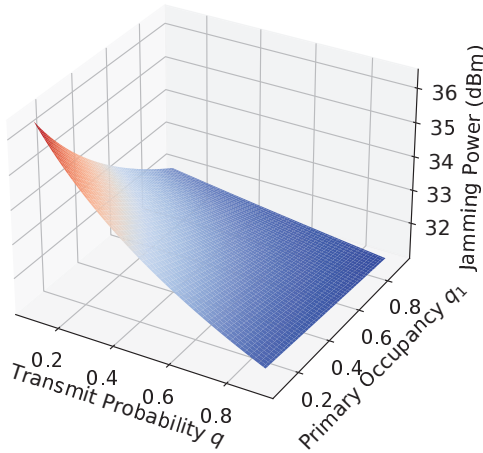


Fig. 7. Jamming power versus channel utilization.

assume the incumbent occupies the channel with probability $q_1 = 0.5$ and show the average AoI with respect to the design parameters the secondary user can select.

Fig. 7 shows the resulting jamming power as a function of channel occupancy by both users. Large transmission probabilities (q) result in more frequent jamming, which requires a reduction in jamming power used per time slot, given the power constraint at the adversary. To some extent, the spectrum sharing yields a reduced interference level from the perspective of each user, since the jammer will use some of its power to cause interference to the other user.

IV. CONCLUSION

We studied the intricate interplay between timeliness and security in NextG spectrum sharing in the presence of an adversary. For this setting, we analyzed the effect of signal classification performance on the selection of jamming power for an adversary with limited resources and evaluated the average AoI. We showed the advantage of sharing the spectrum

when the adversary has limited power budget and will be encouraged to reduce its jamming power with the increased occupancy of the channel. We also considered the effects of the wireless channels and design parameters as the packet size, and show that smaller packets can reduce the average AoI in a scenario of spectrum scarcity under the presence of an adversary. Our findings highlight pathways for developing resilient NextG communications protocols, emphasizing the connection between spectrum sharing, timeliness, and security.

REFERENCES

- [1] M. Matinmikko-Blue, S. Yrjölä, and P. Ahokangas, "Spectrum management in the 6G era: The role of regulation and spectrum sharing," in *IEEE 6G Wireless Summit (6G SUMMIT)*, 2020.
- [2] G. Gür, "Expansive networks: Exploiting spectrum sharing for capacity boost and 6G vision," *Journal of Communications and Networks*, vol. 22, no. 6, pp. 444–454, 2020.
- [3] P. Yang, L. Kong, and G. Chen, "Spectrum sharing for 5G/6G URLLC: Research frontiers and standards," *IEEE communications standards magazine*, vol. 5, no. 2, pp. 120–125, 2021.
- [4] P. Popovski, F. Chiarotti, K. Huang, A. E. Kalør, M. Kountouris, N. Pappas, and B. Soret, "A perspective on time toward wireless 6G," *Proceedings of the IEEE*, vol. 110, no. 8, pp. 1116–1146, 2022.
- [5] S. Kaul, R. Yates, and M. Gruteser, "Real-time status: How often should one update?" in *IEEE INFOCOM*, 2012.
- [6] B. Mao et al., "Security and privacy on 6G network edge: A survey," *IEEE Communications Surveys & Tutorials*, 2023.
- [7] B. Kim, Y. E. Sagduyu, K. Davaslioglu, T. Erpek, and S. Ulukus, "How to make 5G communications "invisible": Adversarial machine learning for wireless privacy," in *Asilomar Conference on Signals, Systems, and Computers*, 2020.
- [8] B. Kim, T. Erpek, Y. E. Sagduyu, and S. Ulukus, "Covert communications via adversarial machine learning and reconfigurable intelligent surfaces," in *IEEE Wireless Communications and Networking Conference (WCNC)*, 2022.
- [9] B. Kim, Y. Sagduyu, K. Davaslioglu, T. Erpek, and S. Ulukus, "Adversarial machine learning for nextg covert communications using multiple antennas," *Entropy*, vol. 24, no. 8, p. 1047, 2022.
- [10] X. Lu et al., "Covert communication with time uncertainty in time-critical wireless networks," *IEEE Transactions on Wireless Communications*, vol. 22, no. 2, pp. 1116–1129, 2023.
- [11] W. Yang, X. Lu, S. Yan, F. Shu, and Z. Li, "Age of information for short-packet covert communication," *IEEE Wireless Communications Letters*, vol. 10, no. 9, pp. 1890–1894, 2021.
- [12] Y. Wang, S. Yan, W. Yang, and Y. Cai, "Covert communications with constrained age of information," *IEEE Wireless Communications Letters*, vol. 10, no. 2, pp. 368–372, 2021.
- [13] M. Costa and Y. E. Sagduyu, "Timely and covert communications under deep learning-based eavesdropping and jamming effects," *Journal of Communications and Networks*, vol. 25, no. 5, pp. 621–630, 2023.
- [14] Y. Xiao and Y. Sun, "A dynamic jamming game for real-time status updates," in *IEEE Conference on Computer Communications (INFOCOM) Workshops*, 2018, pp. 354–360.
- [15] A. Garnaev, W. Zhang, J. Zhong, and R. D. Yates, "Maintaining information freshness under jamming," in *IEEE INFOCOM 2019-IEEE Conference on Computer Communications Workshops (INFOCOM WKSHPS)*, 2019, pp. 90–95.
- [16] S. Banerjee and S. Ulukus, "Age of information in the presence of an adversary," in *IEEE Conference on Computer Communications (INFOCOM) Workshops*, 2022, pp. 1–8.
- [17] E. Fountoulakis, T. Charalambous, N. Nomikos, A. Ephremides, and N. Pappas, "Information freshness and packet drop rate interplay in a two-user multi-access channel," *Journal of Communications and Networks*, vol. 24, no. 3, pp. 357–364, 2022.
- [18] N. E. West and T. O'shea, "Deep architectures for modulation recognition," in *IEEE International Symposium on Dynamic Spectrum Access Networks (DySPAN)*, 2017.
- [19] Y. Shi, K. Davaslioglu, Y. E. Sagduyu, W. C. Headley, M. Fowler, and G. Green, "Deep learning for RF signal classification in unknown and dynamic spectrum environments," in *IEEE International Symposium on Dynamic Spectrum Access Networks (DySPAN)*, 2019.